

Anisotropic polyurethane magnetorheological elastomer prepared through *in situ* polycondensation under a magnetic field

This article has been downloaded from IOPscience. Please scroll down to see the full text article.

2010 Smart Mater. Struct. 19 105007

(<http://iopscience.iop.org/0964-1726/19/10/105007>)

View [the table of contents for this issue](#), or go to the [journal homepage](#) for more

Download details:

IP Address: 202.115.56.163

The article was downloaded on 09/08/2010 at 12:21

Please note that [terms and conditions apply](#).

# Anisotropic polyurethane magnetorheological elastomer prepared through *in situ* polycondensation under a magnetic field

Jinkui Wu<sup>1</sup>, Xinglong Gong<sup>2</sup>, Yanceng Fan<sup>2</sup> and Hesheng Xia<sup>1,3</sup>

<sup>1</sup> State Key Laboratory of Polymer Materials Engineering, Polymer Research Institute of Sichuan University, Chengdu 610065, People's Republic of China

<sup>2</sup> CAS Key Laboratory of Mechanical Behavior and Design of Materials, Department of Modern Mechanics, University of Science and Technology of China, Hefei 230027, People's Republic of China

E-mail: [xiahs@scu.edu.cn](mailto:xiahs@scu.edu.cn)

Received 6 March 2010, in final form 5 July 2010

Published 6 August 2010

Online at [stacks.iop.org/SMS/19/105007](http://stacks.iop.org/SMS/19/105007)

## Abstract

Highly filled polytetramethylene ether glycol (PTMEG)-based polyurethane (PU) magnetorheological elastomers (MREs) with anisotropic structure and good mechanical properties were prepared. The difficulty in dispersion and orientation of iron particles in the PU elastomer was overcome by ball milling mixing and further *in situ* one-step polycondensation under a magnetic field. The microstructure and properties of the composite were characterized in detail. Scanning electron microscopy (SEM) showed that a chain-like structure of carbonyl iron was formed in the PU matrix after orientation under a magnetic field of 1.2 T. The aligned chain-like structure of carbonyl iron in PU greatly enhanced the thermal conductivity, the compression properties and the magnetorheological (MR) effect of anisotropic PU MREs compared to that of the isotropic one. When the test frequency is 1 Hz, the maximum absolute and relative MR effect of anisotropic PU MREs with 26 wt% hard segment and 70 wt% carbonyl iron were  $\sim 1.3$  MPa and  $\sim 21\%$ , respectively.

## 1. Introduction

Magnetorheological elastomers (MREs) belong to a family of so-called smart materials whose rheological properties can be controlled continuously, rapidly and reversibly by the application of an external magnetic field. Generally, it consists of micron-sized magnetic particles suspended in a non-magnetic polymeric matrix. The MRE matrices include silicon rubber [1–6], natural rubber [7–10], synthetic rubber-like nitrile rubber [11, 12], polyurethane (PU) [13–16], and so on. Silicon rubber and natural rubber [1–10] are two kinds of the most common matrices reported in the literature. For silicone rubber, it has many advantages: firstly, it can be simply processed from liquid precursors with low viscosity; secondly, it possesses a higher relative magnetorheological effect for the

low zero-field modulus. However, due to its low strength and reduced fatigue life after loading a high content of magnetic particles, it is still not so good for practical applications [7]. For natural rubber, it has good comprehensive properties as MREs. But its high viscosity during processing makes the magnetic particles difficult to form chain-like structures under a magnetic field. Recently, PU-based MREs [13–16] have attracted a great deal of attention. Typical PU elastomers are (AB)<sub>n</sub>-type multiblock copolymers comprised of alternating soft polyether or polyester polyol segments and hard segments based on isocyanates and chain extender. The properties of PU elastomers, such as tensile strength, stiffness, friction coefficient and chemical resistance, can be easily adjusted by changing the types of soft and hard segments and the content of the hard segments (the weight percentage of the hard segments in PU), etc [17]. PU MREs can be fabricated by either a

<sup>3</sup> Author to whom any correspondence should be addressed.

conventional mixing technique or *in situ* polycondensation from liquid precursors. The PU elastomer is a potential candidate for MREs in practical applications due to its easy processability and adjustable properties.

Previously, we prepared isotropic polyurethane MREs through an *in situ* polycondensation method. The MR test showed that the maximum absolute MR effect and relative MR effect of PU MREs with 70 wt% carbonyl iron were  $\sim 0.3$  MPa and  $\sim 8\%$ , respectively [16]. In this study, we combined the *in situ* one-step polycondensation and magnetic field to prepare anisotropic PU MREs. This method has a potential to be a standard method for MRE fabrication due to the lower viscosity of the prepolymer, resulting in evident anisotropic chain-like structure and a higher magnetorheological effect.

The highly filled PTMEG-based PU MREs with anisotropic structure and good mechanical properties were prepared. The difficulty in dispersion and orientation of iron particles in PU elastomers was overcome by ball milling mixing and further *in situ* one-step polycondensation under a magnetic field. The structure and properties of anisotropic PU MREs were studied in detail.

## 2. Experimental part

### 2.1. Materials

Polytetramethylene ether glycol (PTMEG,  $\bar{M}_n$  is 1000), provided by Mitsubishi Chemical Holdings Corporation, was dehydrated in a vacuum oven at  $110^\circ\text{C}$  for 2 h prior to use. 4,4'-methylene-di (phenylene isocyanate) (MDI), supplied by Yantai Wanhua Polyurethanes Co., Ltd, China, was used as received without further purification. The chain extender 1,4-butanediol (BDO), purchased from Chengdu Kelong Chemical Factory, China, was redistilled to remove water prior to use. The spherical carbonyl iron particles, with a size range of  $3\text{--}5\ \mu\text{m}$ , were produced by Hebao Nanomaterial Co., Ltd, China. The catalyst Dabco-33LV was obtained from Air Products and Chemicals. The antifoam agent BYK-A 506 was provided by Sino Composite Co., Ltd, China.

### 2.2. Preparation of anisotropic polyurethane magnetorheological elastomers

The anisotropic PU MREs with a hard segment content of 26% and 31% were prepared under a magnetic field. The  $\text{--NCO/OH}$  ratio was kept at 1.1:1 for each sample. Carbonyl iron was dispersed in melted PTMEG through ball milling. The prepolymer was obtained by mixing the PTMEG-carbonyl iron (PTMEG-Fe) dispersion with MDI and chain extender BDO. For example, the detailed procedure for anisotropic PU MREs with 26 wt% hard segment and 70 wt% carbonyl iron at a thickness of  $\sim 3$  mm is as follows: the melted PTMEG (30.00 g) and carbonyl iron (94.60 g) were added to the jar and mixed by ball milling for 30 min to obtain the PTMEG-Fe dispersion. The dispersion was blended with 9.98 g of melted MDI, 0.56 g of BDO, 0.03 g of catalyst Dabco-33LV and 0.05 g of antifoam agent BYK-506 at room temperature for 2 min. Then the mixture was vacuum-degassed for 3–5 min to remove the bubbles. After that, the viscous prepolymer was poured



**Figure 1.** The magnetic field apparatus for *in situ* polycondensation. (This figure is in colour only in the electronic version)

into a hot O-ring mold and oriented under a magnetic field of 1.2 T along the thickness direction for 1 h. The dimension of anisotropic PU MRE cylinder samples for compressive tests is 12.5 mm in height and 29.0 mm in diameter, and the samples were prepared under a magnetic field of 0.9 T along the height direction. The magnetic field apparatus for *in situ* polycondensation is shown in figure 1. As the curing reaction between the  $\text{--NCO}$  and  $\text{--OH}$  groups goes on, the viscosity of the prepolymer increases, which fixes the chain-like structure of carbonyl iron in the matrix. Finally, the prepolymer was further cured at  $120^\circ\text{C}$  for 24 h and cooled to room temperature and kept for two weeks to obtain the anisotropic PU MREs. The anisotropic PU MREs with 26 wt% hard segment and 50, 60 and 70 wt% carbonyl iron are designated as Aniso-50, Aniso-60 and Aniso-70, respectively. In contrast, the blank PU and isotropic PU MREs were prepared by the same procedure without a magnetic field. The isotropic PU MREs with 26 wt% hard segment and 50, 60 and 70 wt% carbonyl iron are designated as Iso-50, Iso-60 and Iso-70, respectively. Throughout this paper, if it is not specified as 31%, the hard segment content of the sample is 26 wt%.

### 2.3. Characterization

**2.3.1. Viscosity measurement.** The rheological properties and viscosity of PTMEG-Fe dispersion with different iron contents were investigated by an RH7D rheometer (Bohlin Instruments Ltd) using 40 mm diameter parallel plates. The gap between the plates is 0.15 mm. The sample was allowed to equilibrate for at least 5 min at the test temperature before steady shear measurement. The relationship between viscosity and shear rate was obtained at a shear rate range of  $0.1\text{--}110\ \text{s}^{-1}$  at  $20^\circ\text{C}$ ,  $40^\circ\text{C}$  and  $60^\circ\text{C}$ , respectively.

**2.3.2. Scanning electron microscopy (SEM).** An Inspect F SEM instrument (FEI Company) was used to observe the morphology of the fractured surface and the dispersion of carbonyl iron particles in the matrix with an acceleration

voltage of 10 kV. The samples were cryogenically fractured in liquid nitrogen and coated with a thin gold layer prior to observation.

**2.3.3. Thermal conductivity measurement.** The thermal conductivity of PU and PU MREs was measured on a Hot Disk 2500 thermal constant analyzer, which was based on a transient technique. The measurement was performed by putting a sensor (3 mm in diameter) between two smooth slabs of specimens (50 mm × 50 mm × 3 mm). The sensor supplied a heat pulse of 0.03 W for 10 s to the sample at room temperature and the associated change of temperature was recorded.

**2.3.4. Thermogravimetric analysis (TGA).** TGA was carried out on a Q600 equipment (TA Instrument, USA) in a nitrogen atmosphere to characterize the thermal stability of samples with different carbonyl iron content. The samples were heated from 30 to 700 °C at a heating rate of 10 °C min<sup>-1</sup>.

**2.3.5. Mechanical properties measurement.** The tensile test was performed on an Instron 5567 universal testing instrument at room temperature. The dumbbell-shaped specimens were stretched until breaking at a crosshead rate of 500 mm min<sup>-1</sup>. The tensile strength, elongation and stress at 100%, 200% and 300% strain were the average value of five specimens. For the compression test, the cylinder specimens were compressed to the maximum strain of 25% at a rate of 10 mm min<sup>-1</sup> according to the China Standard GB/T 7757-1993. Four compression cycles were carried out and the last cycle was selected to determine the compressive properties. The dimensions of the cylinder sample are 12.5 mm in height and 29.0 mm in diameter.

**2.3.6. Dynamical mechanical analysis (DMA).** The normal dynamical mechanical test without a magnetic field was performed on a Q-800 instrument (TA Instruments, USA) in dual cantilever mode. The storage modulus ( $E'$ ) and loss factor ( $\tan \delta$ ) were measured in the temperature range of -100–60 °C at a heating rate of 3 °C min<sup>-1</sup>. The strain amplitude was 50  $\mu\text{m}$  and the test frequency was 1 Hz.

**2.3.7. The magnetorheological effect analysis.** The test of the MR effect was conducted on a modified dynamic mechanical analyzer (DMA) (Triton Technology Ltd, UK, model Triton 2000B) [10] at room temperature. A shaft connects the sample and the motor in DMA. The motor drives the shaft and the sample moves at a given amplitude and frequency. The stress in the sample is measured with the sensor and the strain is taken as the displacement amplitude. The shear modulus is computed from the data of strain and stress. During the test, a magnetic field which can vary from 0 to 1000 mT was applied to the sample. The dimensions of the sample are 10 mm × 10 mm × 3 mm. The dynamic strain amplitude was set as 0.3%. The MR effect was tested at three different frequencies, i.e. 1, 5 and 10 Hz.

### 3. Results and discussion

#### 3.1. The rheological behavior of PTMEG-Fe dispersion

The preparation of polyurethane elastomers can be divided into two methods: one step and two step. In the one-step method, diisocyanate, polyol and a chain extender react together. The one-step method has the following advantages: (i) the procedure is simple and (ii) the viscosity of the prepolymer is relatively low. In the two-step method, the prepolymer is first synthesized from diisocyanate and polyol, and then the viscous prepolymer further reacts with a chain extender. In the latter, the viscosity of the prepolymer increases significantly, which makes it difficult to remove the bubbles from the prepolymer. So in this study we choose the one-step method to prepare the PU MREs. The introduction of the micron-sized carbonyl iron has a significant influence on the viscosity of the PTMEG-Fe dispersion, which will further affect the orientation of iron in the PU matrix. So we tested the viscosity of the PTMEG-Fe dispersion prior to curing. The effects of the shear rate, carbonyl iron content and temperature on the viscosity of the PTMEG and PTMEG-Fe dispersion are shown in figure 2. The data can be fitted well with the Herschel–Bulkley model:  $\eta = \tau_0/\dot{\gamma} + k\dot{\gamma}^{n-1}$  [18], where  $\dot{\gamma}$  is the shear rate,  $k$  and  $\tau_0$  are constants, and  $n$  is the flow behavior index or shear thinning parameter. The viscosity at a low shear rate of 1.10 s<sup>-1</sup> and a high shear rate of 70.00 s<sup>-1</sup>, and the fitted shear thinning parameter  $n$  are listed in table 1. The blank PTMEG exhibits a Bingham fluid behavior, while the PTMEG-Fe dispersion shows a pseudoplastic behavior, i.e. shear thinning behavior. With the increase of the iron content, the viscosity of the PTMEG-Fe dispersion increases significantly. For example, at a shearing rate of 1.10 s<sup>-1</sup>, the viscosity of the PTMEG-Fe dispersions for Aniso-50, Aniso-60 and Aniso-70 at 40 °C are 1.38, 4.39 and 87.66 Pa s, respectively. Also the shear thinning parameter  $n$  shows an obvious decrease from 0.87 to 0.51. So, for the PTMEG-Fe dispersion, the higher the carbonyl iron content is, the more obvious the shear thinning behavior is. Temperature also has a great influence on the viscosity of the dispersion. When the temperature increased from 20 to 60 °C, the viscosity of the PTMEG-Fe dispersion for Aniso-60 at a shearing rate of 70.00 s<sup>-1</sup> reduced sharply from 7.96 to 0.98 Pa s, and the shear thinning parameter  $n$  decreased slightly. The sensitivity of PTMEG-Fe viscosity to the shear rate and temperature can be utilized in the sample preparation process. High temperature and vigorous stirring will lead to a low viscosity and the complete mixing of the PTMEG-Fe dispersion.

#### 3.2. The morphology of carbonyl iron in PU matrix

The SEM images of the cryogenically fractured surface of isotropic and anisotropic PU MREs are shown in figure 3. For isotropic PU MREs, the carbonyl iron particles were dispersed randomly in the PU matrix (figures 3(a) and (b)): no large aggregates can be seen in the fractured surface even when the iron content is as high as 70 wt%. For anisotropic PU MREs, after orientation under a magnetic field of 1.2 T, the carbonyl iron particles formed a chain-like structure along the direction

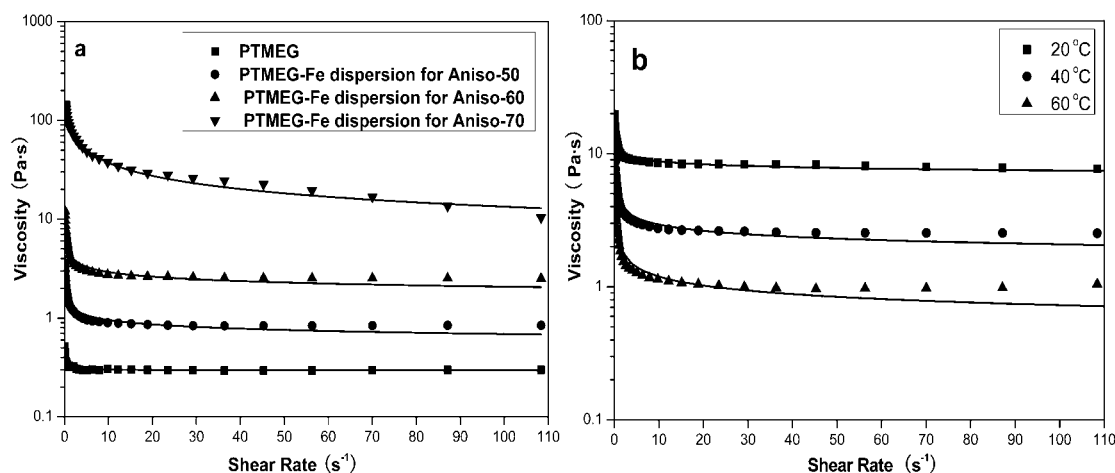


**Figure 2.** The influence of iron content on the viscosity of PTMEG-Fe dispersion at a temperature of 40 °C (a) and the effect of temperature on the viscosity of PTMEG-Fe dispersion for PU MREs with 60 wt% carbonyl iron (b).

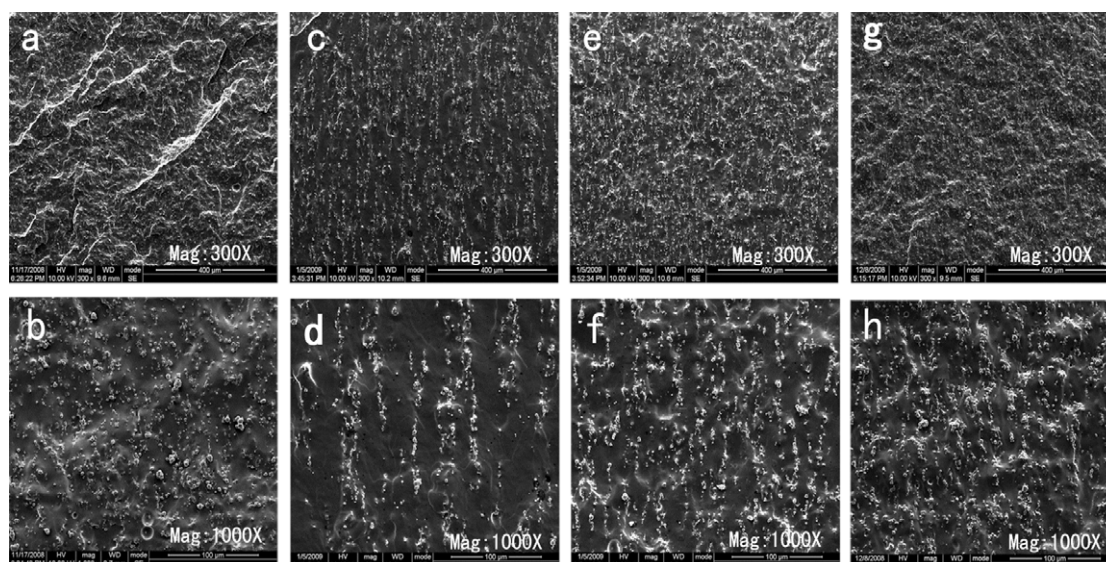


**Figure 3.** The SEM photos of fractured surface of isotropic PU MREs with 70 wt% carbonyl iron (a) and (b), anisotropic PU MREs with different carbonyl iron contents: (c) and (d) with 50 wt% iron, (e) and (f) with 60 wt% iron, and (g) and (h) with 70 wt% iron.

**Table 1.** The viscosity at a low shear rate of  $1.10 \text{ s}^{-1}$  ( $\eta_L$ ) and a high shear rate of  $70.00 \text{ s}^{-1}$  ( $\eta_H$ ) and shear thinning parameter  $n$ .

Dispersion	Test temperature	$\eta_L$ (Pa s)	$\eta_H$ (Pa s)	$n$
	(°C)			
PTMEG	40	0.33	0.30	$1.00 \pm 0.004$
Aniso-50	40	1.38	0.84	$0.87 \pm 0.019$
Aniso-60	20	10.39	7.96	$0.94 \pm 0.009$
Aniso-60	40	4.39	2.54	$0.86 \pm 0.019$
Aniso-60	60	2.05	0.98	$0.80 \pm 0.023$
Aniso-70	40	87.66	16.72	$0.51 \pm 0.007$

of the magnetic field. When the magnetic field is applied to the prepolymer, the interaction among the iron particles makes them align along the magnetic field. As the curing reaction goes on, the chain-like structure of the carbonyl iron is locked in the matrix. From figures 3(c) and (d), it can be noted that the carbonyl iron particles form parallel chains in the PU matrix

with 50 wt% iron, and the gap between the adjacent chains is quite wide. When the iron content is 60 wt% (figures 3(e) and (f)), the chains become dense and the chain gap decrease. Further increasing the iron content to 70 wt%, the chains become denser, but the chain-like structure is not so obvious compared to that with a lower iron content. This should be attributed to the higher viscosity of the PTMEG-Fe dispersion for Aniso-70 PU MREs (see figure 2). Compared to the natural rubber MRE system [7], the chain-like structure of PU MREs with 70 wt% iron is more evident as the orientation of iron particles in the liquid PU prepolymer is much easier than that in the solid natural rubber matrix.

### 3.3. Thermal properties

Figure 4 shows the thermal conductivity of PU, isotropic and anisotropic PU MREs with different carbonyl iron contents. The thermal conductivity of blank PU is only  $\sim 0.23 \text{ W mk}^{-1}$ .

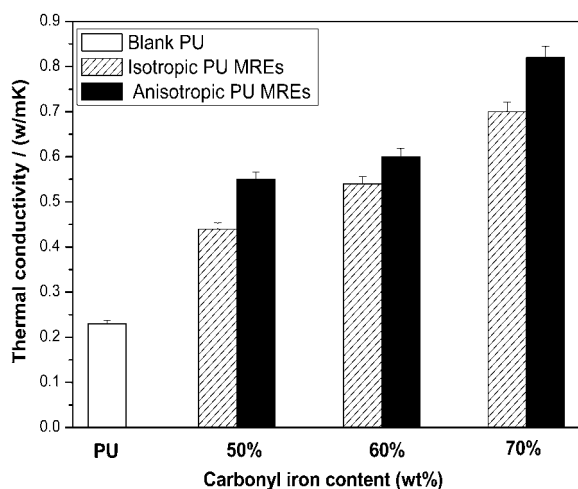


**Figure 4.** The thermal conductivity of PU, isotropic and anisotropic PU MREs with different iron contents.

When the iron content is 70 wt%, the thermal conductivity of isotropic PU MREs increases to  $\sim 0.70 \text{ W mK}^{-1}$ , three times that of blank PU. This is the direct result of incorporating carbonyl iron with high thermal conductivity into the PU matrix. For anisotropic PU MREs, the thermal conductivity increased more compared with the isotropic one. For example, the thermal conductivity of Aniso-70 reached  $\sim 0.82 \text{ W mK}^{-1}$ . The chain-like structure of carbonyl iron in the PU matrix can act as a heat transfer pathway.

The TGA curves of PU and anisotropic PU MREs with different carbonyl iron contents in the nitrogen atmosphere and the characteristic thermal decomposition temperature are shown in figure 5 and table 2, respectively. In general, the thermal degradation of polyurethane occurs in two stages: the initial degradation stage I is primarily the decomposition of the hard segment, which involves the dissociation of urethane into the original polyol and isocyanate, which then forms a primary amine, alkene and carbon dioxide. Stage I is influenced by the hard segment content. The consequent stage II proceeds by the depolycondensation and polyol degradation mechanisms, and is affected by the soft segment content [19]. The thermal decomposition temperature for PU and PU MREs in a nitrogen atmosphere is shown in table 2.  $T_{\text{onset}}$  and  $T_{\text{end}}$  represent the temperature at which the degradation of the PU matrix starts and ends,  $T_{\text{max1}}$  and  $T_{\text{max2}}$  are the temperature with the maximal thermal degradation rate in stage I and stage II, respectively. In a nitrogen atmosphere, the mass of carbonyl iron particles was almost constant during heating and so the mass loss of PU MREs was entirely due to the thermal degradation of the PU matrix. From table 2, it can be seen that, with the incorporation of carbonyl iron,  $T_{\text{onset}}$  and  $T_{\text{max1}}$  decreased. The possible explanations are as follows: the increase of the thermal conductivity of composites leads to the faster degradation of the PU matrix; furthermore, iron can catalyze the decomposition and thereby accelerate the oxidation. The carbonyl iron has little effect on the  $T_{\text{max2}}$  and  $T_{\text{end}}$ . The high carbonyl iron content reduces the thermal stability of PU MREs, which is in agreement with the results based on natural rubber MREs reported by Lokander *et al* [20].

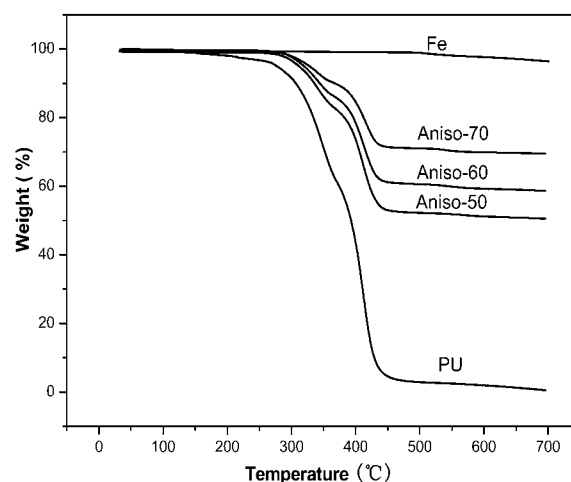


**Figure 5.** TGA curves of PU, carbonyl iron and anisotropic PU MREs with different carbonyl iron contents.

**Table 2.** The thermal decomposition temperature of PU and anisotropic PU MREs in a nitrogen atmosphere.

Sample	$T_{\text{onset}}$ (°C)	$T_{\text{max1}}$ (°C)	$T_{\text{max2}}$ (°C)	$T_{\text{end}}$ (°C)
PU	308.8	354.1	416.8	432.6
Anio-50	293.5	341.5	411.8	431.7
Anio-60	293.0	339.3	412.2	432.8
Anio-70	284.8	338.1	417.2	434.4

### 3.4. Mechanical properties

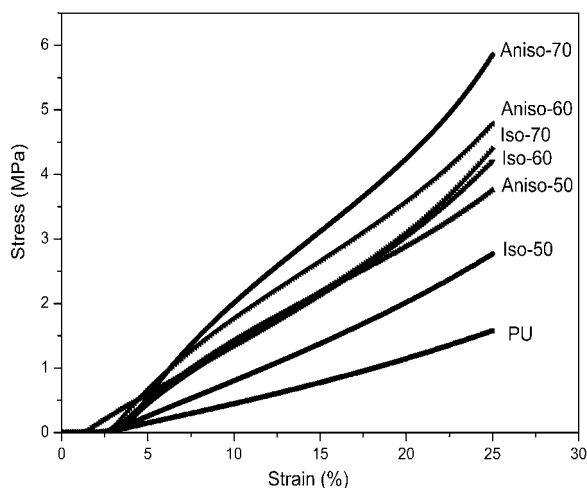
In order to obtain a good MR effect, the high content of magnetic particles for MREs is necessary. In such a case, the mechanical properties become worse and cannot meet the requirements of practical applications. From the viewpoint of practical use, both mechanical and magnetorheological properties are very important: during the long-term service, a balance between the two properties should be considered.

The compressive stress–strain curves of blank PU, isotropic as well as anisotropic PU MREs oriented under a magnetic field of 0.9 T during the curing process with different carbonyl iron contents are shown in figure 6. At low strains, the stress is zero. It is caused by the relaxation of the polymer chain during the first three compression cycles. With the incorporation of iron particles, the compression stress was significantly improved. The compression stress at a strain of 10% for Aniso-70 is 2.02 MPa,  $\sim 4.5$  times that of blank PU (0.45 MPa). Clearly, compared to the isotropic PU MREs, the anisotropic one has a higher compression stress. The reason should be attributed to the orientation of iron particles along the direction of compression.

The tensile properties of PU, Aniso-50, Aniso-60 and Aniso-70 are shown in table 3. It can be seen that the tensile strength decreases with the increasing iron content. But the tensile strength of PU MREs with 70 wt% iron can still be as high as 8.33 MPa,  $\sim 3.5$  times that of natural rubber MREs, which was 2.27 MPa with the same iron content [10]. The deterioration of the mechanical properties of PU MREs can be explained as follows: firstly, the tensile load transfer is

**Table 3.** Mechanical properties of anisotropic PU MREs with different carbonyl iron contents.

Sample	Tensile strength (MPa)	Elongation at break (%)	Stress at 100% strain (MPa)	Stress at 200% strain (MPa)	Stress at 300% strain (MPa)
PU	18.21 ± 0.28	514 ± 16.92	1.95	2.34	2.96
Aniso-50	10.55 ± 2.55	455 ± 45.18	2.75	3.87	5.44
Aniso-60	9.79 ± 1.57	503 ± 5.23	3.22	4.49	6.03
Aniso-70	8.33 ± 0.47	477 ± 0.86	4.50	6.00	6.91

**Figure 6.** The compressive stress–strain curves of isotropic and anisotropic PU MREs with different carbonyl iron contents.

poor at high iron content; and secondly, the oriented chain-like structure in the PU matrix may act as stress concentration points.

Figure 7 shows the DMA (to distinguish from the MR effect, the DMA was tested without a magnetic field) of blank PU and anisotropic PU MREs with different carbonyl iron contents. The  $\tan \delta$  peak is associated with the soft segment glass transition temperature ( $T_g$ ) of PU, which is  $\sim -20^\circ\text{C}$ . Below the glass transition temperature, the effect of iron content on the storage modulus is not obvious. Above room temperature, the storage modulus increases with increasing the iron content. The incorporation of rigid iron and the formation of a chain-like structure raised the stiffness of the composites. The  $\tan \delta$  represents the ratio of the viscous part to the elastic part (energy loss/energy stored) of the material. The  $\tan \delta$  of the PU elastomer is as high as  $\sim 0.90$ , suggesting the hysteresis loss is very evident. With the incorporation of iron, the loss factor corresponding to  $\alpha$  relaxation decreased. For example, the  $\tan \delta$  of Aniso-70 decreased to  $\sim 0.65$ , while the  $\tan \delta$  peak width did not change apparently. This result indicates that the increased filler content contributed mainly to the increase in the elastic component of the composites. This result agrees with the usually observed behavior in filled rubber composites [21].

### 3.5. Magnetorheological effect

The MR effect originates from the interaction of magnetic particles. When MREs are subjected to a magnetic field, magnetic particles tend to align in the direction of the magnetic field in that ferrous particles can be magnetized easily. The

field-induced magnetic forces between the magnetic particles provide an ability of anti-deformation, resulting in the change of shear modulus. In this study, the factors affecting the MR effect of the PU MREs, including the aggregate structure of magnetic particles, the hardness of the matrix, the test frequency and the magnetic particles content, were studied.

Figure 8(a) is the MR effect of isotropic and anisotropic PU MREs oriented under 1.2 T with 70 wt% carbonyl iron tested at 1 Hz. Here,  $G_0$  is the zero-field shear modulus,  $\Delta G$  is the increment of field-induced shear modulus, i.e. absolute MR effect, and  $\Delta G/G_0 \times 100\%$  is the relative MR effect. The zero-field moduli of isotropic and anisotropic PU MREs are  $\sim 3.8$  and  $\sim 6.1$  MPa, respectively. The orientation of iron particles resulted in a  $\sim 60\%$  increase of the zero-field modulus as the orientation further enhanced the rigidity of the composite. The absolute MR effect of Iso-70 and Aniso-70 is  $\sim 0.3$  MPa and  $\sim 1.3$  MPa, and the relative MR effect is 8.0% and 21.0%, respectively. It is obvious that the orientation of the iron in the PU matrix greatly improves the MR effect. After orientation, the formed chain-like structure is locked in the PU matrix. The alignment of carbonyl iron reduces the distance of the iron particles, which can enhance the interaction of iron particles under a magnetic field.

The hardness of PU elastomers can be adjusted easily by changing the hard segment content. With a higher hard segment content, the content of the soft segment is lower, thus the molecules become rigid. The MR effect of anisotropic PU MREs with hard segments of 26 and 31 wt% is shown in figure 8(b). As can be seen, the zero-field modulus changed from  $\sim 6.1$  to  $\sim 9.9$  MPa, increased by  $\sim 62\%$  with a variation of the hard segment content from 26 to 31 wt%. However, the absolute MR effect remains unchanged, which means the increase of the hard segment of the PU matrix has no influence on the absolute MR effect. At the same time, the relative MR effect reduces from 21% to 13% for the increasing of the zero-field modulus. So by changing the hard segment content of the PU matrix, the relative MR effect can be adjusted.

The frequency dependence of the MR effect of the PU elastomers was investigated. The MR effect of Aniso-70 at 1, 5 and 10 Hz is shown in figure 8(c). It can be noted that the zero-field modulus increases with increasing the test frequency. This should be attributed to the frequency dependence of the polymer matrix. With an increase in the frequency, the motion of PU molecular chains cannot keep up with the external stimuli. The molecular chains tend to be rigid which results in an enhancement of the zero-field modulus. Increasing the frequency has no influence on the absolute MR effect but will lower the relative MR effect. So the operating frequency should be considered in the application of MREs.

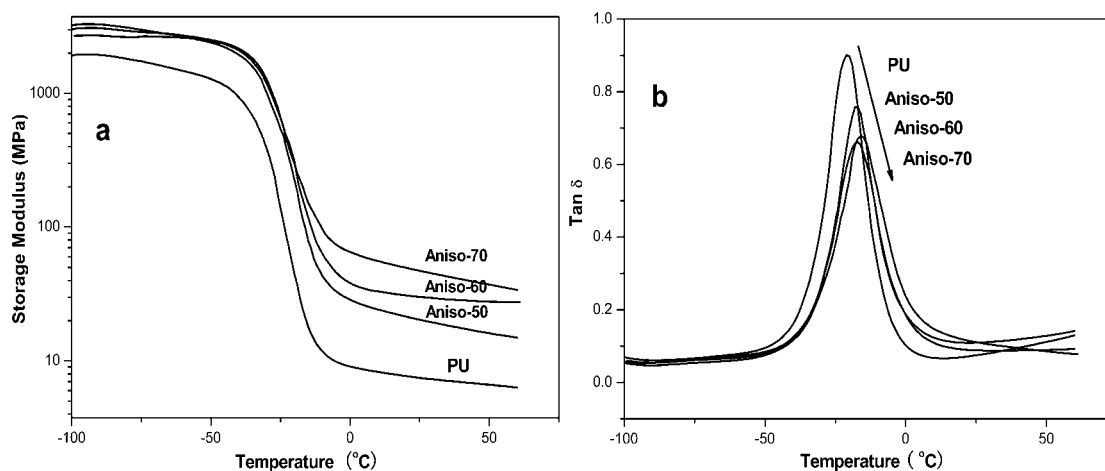


Figure 7. The storage modulus (a) and loss factor (b) of anisotropic PU MREs.

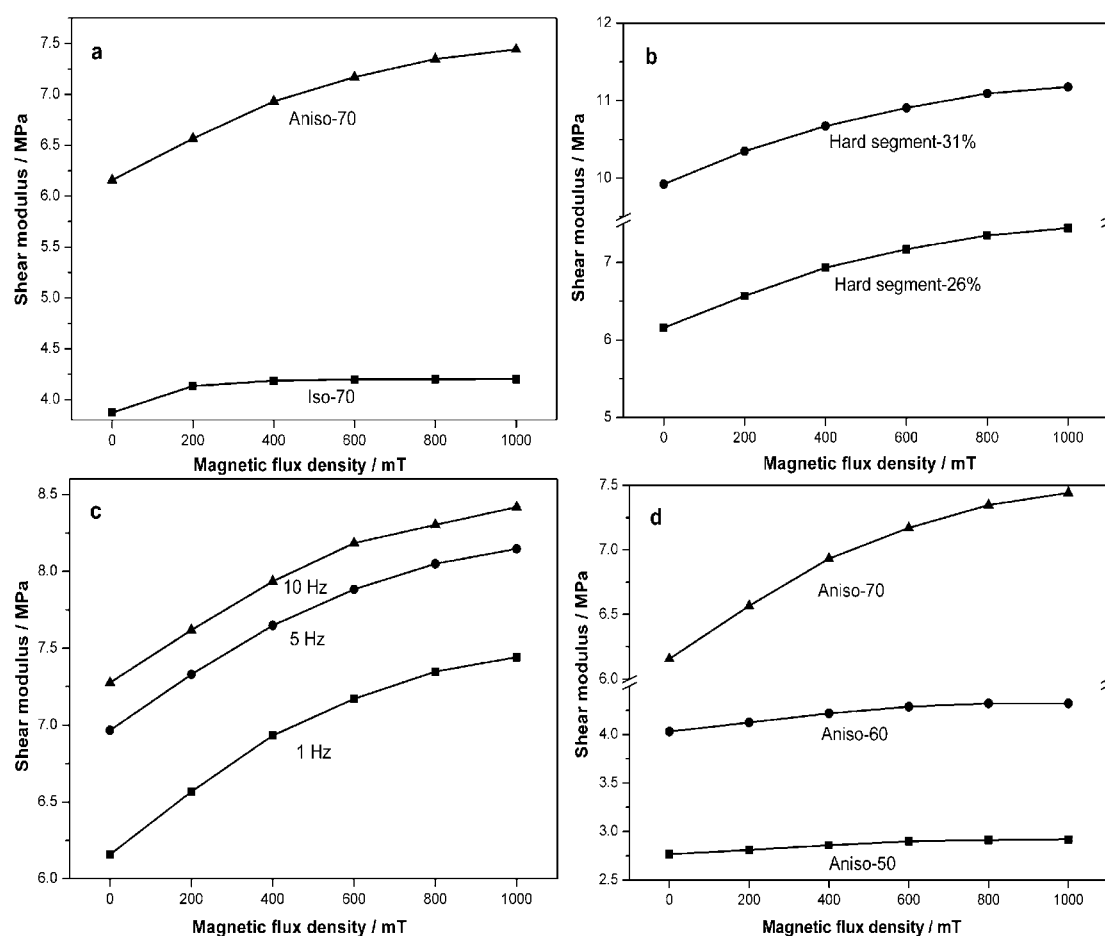


Figure 8. Magnetic-field-induced shear modulus increment of (a) isotropic and anisotropic PU MRE with 70 wt% carbonyl iron tested at 1 Hz, (b) anisotropic PU MRE with 26% and 31% of hard segments, the carbonyl iron content is 70 wt%, tested at 1 Hz, (c) anisotropic PU MRE with 70 wt% carbonyl iron tested at 1, 5 and 10 Hz, and (d) anisotropic PU MRE with different carbonyl iron contents at 1 Hz.

Figure 8(d) illustrates the MR effect of anisotropic PU MREs with different carbonyl iron contents. The MR effect appears when the content of carbonyl iron particles is 50 wt%, and becomes relatively pronounced at an iron content of 70 wt%. The absolute MR effect of Aniso-50, Aniso-60 and Aniso-70 is  $\sim 0.2$  MPa,  $\sim 0.3$  MPa and  $\sim 1.3$  MPa, respectively.

The significant difference in the MR effect with different iron contents can be ascribed to the chain-like microstructure in the PU matrix. The chain-like structure in the PU matrix with 70 wt% carbonyl iron is the densest, so the interaction between iron particles under a magnetic field is the strongest. In the previous studies, the maximum absolute MR effect for

silicon MREs [22] is  $\sim 0.6$  MPa with 30 vol.% ( $\sim 75$  wt%) of iron and for natural rubber MREs [7] is  $\sim 0.9$  MPa with 40 vol.% ( $\sim 83$  wt%) of iron. Compared to those systems, PU MREs in the present study have a higher MR effect. This can be attributed to the low viscosity of PU prepolymer through *in situ* one-step polycondensation, which makes the iron easily oriented under the magnetic field.

#### 4. Conclusion

The highly filled PTMEG-based polyurethane magnetorheological elastomers with anisotropic structure and good mechanical properties were prepared by a *in situ* one-step polycondensation process under a magnetic field. The influences of carbonyl iron particle content on the microstructure, thermal, mechanical and MR properties of PU MREs were investigated. The results confirmed that PU is a good matrix for MREs.

- (1) Through magnetic-field-induced orientation during the *in situ* polycondensation process of polyurethane, the formed chain-like structure of carbonyl iron particles is locked in the PU matrix. The chain-like structure becomes denser as the iron content increases.
- (2) The orientation of carbonyl iron particles can greatly enhance the compressive strength of the composite, but the tensile properties of PU MREs decrease. However, with a hard segment of 26 wt% and an iron content of 70 wt%, the tensile strength and elongation at break of PU MREs can still remain at 8.33 MPa and 477%, respectively.
- (3) The MR test shows that the maximum absolute MR effect and relative MR effect of anisotropic PTMEG-based PU MREs are  $\sim 1.3$  MPa and  $\sim 21\%$  at 1 Hz with a hard segment of 26 wt% and an iron content of 70 wt%. The MR effect increases with increasing the iron content. With an increase in the hard segment content of PU and the test frequency, the relative MR effect decreases, but the absolute MR effect changes slightly.

#### Acknowledgments

This work was supported by the National Science Foundation of China (50673060) and the National Basic Research Program of China (973 Program, no. 2007CB714701).

#### References

- [1] Varga Z, Filipcsei G and Zrnfiy M 2005 Smart composites with controlled anisotropy *Polymer* **46** 7779–87
- [2] Varga Z, Filipcsei G and Zrnfiy M 2006 Magnetic field sensitive functional elastomers with tuneable elastic modulus *Polymer* **47** 227–33
- [3] Kchit N and Bossis G 2008 Piezoresistivity of magnetorheological elastomers *J. Phys.: Condens. Matter* **20** 2041361
- [4] Wilson M J, Fuchs A and Gordaninejad F J 2002 Development and characterization of magnetorheological polymer gels *Appl. Polym. Sci.* **84** 2733–42
- [5] Zhou G Y 2003 Shear properties of a magnetorheological elastomer *Smart Mater. Struct.* **12** 139–46
- [6] Kallio M, Lindroos T, Aalto S, Jarvinen E, Karna T and Meinander T 2007 Dynamic compression testing of a tunable spring element consisting of a magnetorheological elastomer *Smart Mater. Struct.* **16** 506–14
- [7] Ginder J M, Nichols M E, Elie L D and Tardiff J L 1999 Magnetorheological elastomers: properties and applications *Proc. SPIE* **3675** 131–8
- [8] Ginder J M, Nichols M E, Elie L D and Clark S M 2000 Controllable-stiffness components based on magnetorheological elastomers *Proc. SPIE* **3985** 418–25
- [9] Shen Y, Golnaraghi M F and Heppler G R 2004 Experimental research and modeling of magnetorheological elastomers *J. Intell. Mater. Syst. Struct.* **15** 27–35
- [10] Chen L, Gong X L, Jiang W Q, Yao J J, Deng H X and Li W H 2007 Investigation on magnetorheological elastomers based on natural rubber *J. Mater. Sci.* **42** 5483–9
- [11] Lokander M and Stenberg B 2003 Performance of isotropic magnetorheological rubber materials *Polym. Test.* **22** 245–51
- [12] Lokander M and Stenberg B 2003 Improving the magnetorheological effect in isotropic magnetorheological rubber materials *Polym. Test.* **22** 677–80
- [13] Boczkowska A, Awietjan S, Babski K, Wroblewski R and Leonowicz M 2006 Effect of the processing conditions on the microstructure of urethane magnetorheological elastomers *Proc. SPIE* **6170** 61700R
- [14] Boczkowska A, Awietjan S and Wroblewski R 2007 Microstructure-property relationships of urethane magnetorheological elastomers *Smart Mater. Struct.* **16** 1924–30
- [15] Fuchs A, Zhang Q, Elkins J, Gordaninejad F and Evrinsel C 2007 Development and characterization of magnetorheological elastomers *J. Appl. Polym. Sci.* **105** 2497–508
- [16] Wu J K, Gong X L, Chen L, Xia H S and Hu Z G 2009 Preparation and characterization of isotropic polyurethane magnetorheological elastomer through *in situ* polymerization *J. Appl. Polym. Sci.* **114** 901–10
- [17] Furukawa M, Mitsui Y, Fukumaru T and Kojio K 2005 Microphase-separated structure and mechanical properties of novel polyurethane elastomers prepared with ether based diisocyanate *Polymer* **46** 10817–22
- [18] Xia H S and Song M 2006 Preparation and characterisation of polyurethane grafted single-walled carbon nanotubes and derived polyurethane nanocomposites *J. Mater. Chem.* **16** 1843–51
- [19] Bajsić E G and Rek V 2001 Thermal stability of polyurethane elastomers before and after UV irradiation *J. Appl. Polym. Sci.* **79** 864–73
- [20] Lokander M, Reitberger T and Stenberg B 2004 Oxidation of natural rubber-based magnetorheological elastomers *Polym. Degrad. Stab.* **86** 467–71
- [21] Yan N, Wu J K, Zhan Y H and Xia H S 2009 Carbon nanotubes/carbon black synergistic reinforced natural rubber composites *Plast. Rubber Compos.* **38** 290–6
- [22] Jolly M R, Carlson J D and Munoz B C 1996 A model of the behaviour of magnetorheological materials *Smart Mater. Struct.* **5** 607–14